

# Strongly Gapped Spin-Wave Excitation in the Insulating Phase of NaOsO<sub>3</sub>

S. Calder,<sup>1,\*</sup> J. G. Vale,<sup>2,3,†</sup> N. Bogdanov,<sup>4</sup> C. Donnerer,<sup>2</sup> M. Moretti Sala,<sup>5</sup> X. Liu,<sup>6,7</sup> M. H. Upton,<sup>8</sup> D. Casa,<sup>8</sup> Y. G. Shi,<sup>9,10</sup> Y. Tsujimoto,<sup>11</sup> K. Yamaura,<sup>10,12</sup> J. P. Hill,<sup>6</sup> J. van den Brink,<sup>4</sup> D. F. McMorrow,<sup>2</sup> and A. D. Christianson<sup>1,13</sup>

<sup>1</sup>*Quantum Condensed Matter Division, Oak Ridge National Laboratory, Oak Ridge, Tennessee 37831, USA*

<sup>2</sup>*London Centre for Nanotechnology and Department of Physics and Astronomy, University College London, Gower Street, London, WC1E 6BT, United Kingdom*

<sup>3</sup>*Laboratory for Quantum Magnetism, Ecole Polytechnique Fédérale de Lausanne (EPFL), CH-1015, Switzerland*

<sup>4</sup>*Institute for Theoretical Solid State Physics, IFW Dresden, D01171 Dresden, Germany*

<sup>5</sup>*European Synchrotron Radiation Facility, BP 220, F-38043 Grenoble Cedex, France*

<sup>6</sup>*Condensed Matter Physics and Materials Science Department, Brookhaven National Laboratory, Upton, NY 11973, USA*

<sup>7</sup>*Beijing National Laboratory for Condensed Matter Physics and Institute of Physics, Chinese Academy of Sciences, Beijing 100190, China*

<sup>8</sup>*Advanced Photon Source, Argonne National Laboratory, Argonne, Illinois 60439, USA*

<sup>9</sup>*Institute of Physics, Chinese Academy of Sciences, 100190 Beijing, China.*

<sup>10</sup>*Superconducting Properties Unit, National Institute for Materials Science, 1-1 Namiki, Tsukuba, 305-0044 Ibaraki, Japan.*

<sup>11</sup>*International Center for Materials Nanoarchitectonics (MANA),*

*National Institute for Materials Science, Tsukuba, Ibaraki 305-0044, Japan.*

<sup>12</sup>*JST, Transformative Research-Project on Iron Pnictides (TRIP), 1-1 Namiki, Tsukuba, 305-0044 Ibaraki, Japan.*

<sup>13</sup>*Department of Physics and Astronomy, University of Tennessee, Knoxville, TN 37996, USA*

NaOsO<sub>3</sub> hosts a rare manifestation of a metal-insulator transition driven by magnetic correlations, placing the magnetic exchange interactions in a central role. We use resonant inelastic x-ray scattering to directly probe these magnetic exchange interactions. A dispersive and strongly gapped (58 meV) excitation is observed indicating appreciable spin-orbit coupling in this 5d<sup>3</sup> system. The excitation is well described within a minimal model Hamiltonian with strong anisotropy and Heisenberg exchange ( $J_1 = J_2 = 13.9$  meV). The observed behavior places NaOsO<sub>3</sub> on the boundary between localized and itinerant magnetism.

The underlying mechanisms driving a metal-insulator transition (MIT) has been an enduring focus of condensed matter physics [1]. Recent interest has extended investigations to 5d-based transition metal oxides that host new paradigms of competing interactions creating novel MITs [2]. For example spin-orbit coupling (SOC) in 5d<sup>5</sup> iridates dramatically influences their behavior driving a relativistic Mott MIT, even in the presence of reduced on-site Coulomb interaction ( $U$ ) [3]. In 5d<sup>3</sup> osmium-based compounds MITs occur that cannot be reconciled with the Mott approximation and have required the invocation of novel mechanisms. Of particular interest in this regard are the osmates NaOsO<sub>3</sub> and Cd<sub>2</sub>Os<sub>2</sub>O<sub>7</sub> which undergo a MIT that is continuous and coincident with the onset of magnetic order [4–7].

Slater considered such a magnetically driven MIT with the central observation being that within a magnetically ordered system the potential created by an up-spin is different from that created by a down-spin [8]. By this definition three-dimensional magnetic ordering with oppositely aligned spins is a route to a MIT, and implicitly includes  $q=0$  antiferromagnetic structures. NaOsO<sub>3</sub> exhibits several features consistent with Slater’s general scenario [6, 7, 9–13]. The MIT occurs concomitant with the onset of antiferromagnetic ordering ( $T_N = T_{MIT} = 410$  K) that can create a periodic potential. Furthermore in NaOsO<sub>3</sub> the MIT is continuous and no struc-

tural symmetry change occurs. However several important questions have so far remained experimentally inaccessible hindering the development of further insight into the mechanism of this unusual MIT and prohibiting a quantitative description beyond the mean-field approach invoked by Slater for a magnetic MIT.

Principally, since the MIT is driven by magnetic ordering the magnetic exchange interactions ( $J$ ) are central to the creation of the MIT in NaOsO<sub>3</sub>. Therefore measuring the dominant exchange pathways and interactions is required to build robust models of the MIT. Additionally the energy scales of the interactions that are required to describe the electronic behavior, such as crystal field splitting, Hund’s coupling and SOC have not been accessed. In particular the nominal 5d<sup>3</sup> electronic occupancy suggests zero orbital angular momentum in the  $L-S$  coupling limit and previous experimental descriptions did not require the inclusion of strong SOC. However, mounting experimental evidence in other 5d<sup>3</sup> systems indicates SOC is required to describe the magnetism [14–16]. To answer these questions we performed resonant inelastic x-ray scattering (RIXS) to directly probe the 5d electrons of the Os ion in NaOsO<sub>3</sub>.

RIXS measurements at the Os L<sub>3</sub>-edge (10.87 keV) were performed on the ID20 spectrometer at the ESRF, Grenoble. A single crystal of NaOsO<sub>3</sub> was oriented with the (HOL) plane normal to the sample surface. The scat-

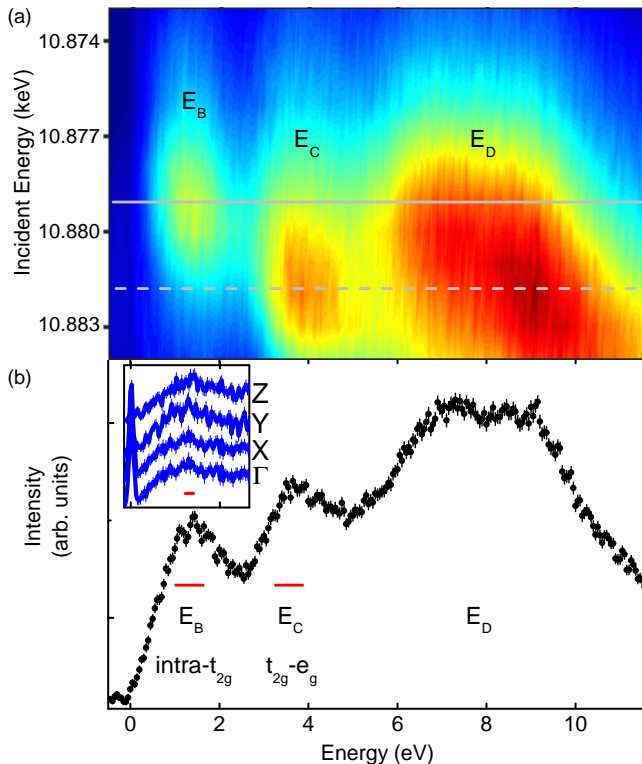


FIG. 1. (a) Excitations measured in  $\text{NaOsO}_3$  at various fixed incident energies through the Os L-edge using RIXS. Three inelastic peaks are observed labeled  $E_B$ ,  $E_C$  and  $E_D$ . The solid (dashed) gray line indicates the incident energy that yields the maximum intensity for  $E_B$  ( $E_C$ ). (b) RIXS measurement at fixed incident energy of 10.88 keV. Main panel was measured with a resolution of  $\Delta E=275$  meV and the inset data was collected with  $\Delta E=46$  meV. The horizontal red lines indicate the FWHM experimental resolution.

tering plane and incident photon polarization were both horizontal, i.e.  $\pi$  incident polarization, with the incident beam focused to a size of  $20 \times 10 \mu\text{m}^2$  ( $H \times V$ ) at the sample position. Low resolution measurements with a Si(311) channel-cut secondary monochromator provided information on the orbital excitations, whereas a (664) four-bounce high-resolution setup allowed examination of the low-energy magnetic excitations. Both of these setups used a Si(664) diced spherical analyzer (2m radius) to reflect the scattered photons towards a Maxipix CCD detector (pixel size  $\sim 55 \mu\text{m}$ ). The total energy resolution for the low and high-resolution setups were determined to be  $\Delta E=275$  meV and  $\Delta E = 46$  meV respectively, based on scattering from a charge peak. Preliminary measurements were performed at the Advanced Photon Source (APS) on the MERIX instrument using an identical setup to that described in Ref. 16.

A RIXS map of the orbital excitations ( $d-d$  transitions) in  $\text{NaOsO}_3$  obtained by measuring the inelastic energy loss spectrum at several fixed incident energies through

the Os resonant edge is shown in Fig. 1(a) at 300 K. Three broad inelastic features are observed, labeled  $E_B$ ,  $E_C$  and  $E_D$ . On a qualitative level the excitations appear analogous to RIXS measurements on  $5d^3$ -based  $\text{Cd}_2\text{Os}_2\text{O}_7$  [16] and exhibit notable differences from measurements of  $5d^5$  based iridates [17]. The incident energy dependence of features  $E_B$  and  $E_C$  in the RIXS map is consistent with a nominal splitting of the  $5d$  manifold into states with  $t_{2g}$  and  $e_g$  symmetry with the scattering following dipole selection rules ( $\Delta S = 1$ ).  $E_B$  involves intra- $t_{2g}$  transitions whereas  $E_C$  is due to  $t_{2g}-e_g$  excitations. We assign excitation  $E_D$  to ligand-metal charge transfer (LMCT).

The inelastic excitation  $E_B$  is centered at 1.27(2) eV and corresponds to intra- $t_{2g}$  transitions. As shown in the inset of Fig. 1(b) even when measured with the high-resolution RIXS set-up  $E_B$  remained as a broad single-peaked excitation, significantly broader than resolution (46 meV).  $E_B$  therefore reveals no well defined splitting of the  $t_{2g}$  manifold in  $\text{NaOsO}_3$ . This contrasts to the case of the iridium-based relativistic Mott insulators, where SOC strongly splits the  $t_{2g}$  electronic ground state into  $J_{\text{eff}}=1/2$  and  $J_{\text{eff}}=3/2$  bands and results in a measured splitting of  $E_B$  [17, 18]. Since  $E_B$  consists of intra- $t_{2g}$  transitions we follow the reasoning outlined in Ref. 16 to experimentally define the Hund's coupling energy ( $J_H$ ) value in  $\text{NaOsO}_3$  as  $J_H=1.27 \text{ eV}/3.75=0.34 \text{ eV}$  based on the centre of  $E_B$ . The 3.75 factor derives from the consideration of  $E_B$  as consisting of eight  $S=1/2$  states, five of which have relative energy  $3J_H$  and three having  $5J_H$  yielding an average of  $3.75J_H$ . Excitation  $E_C$  is located at 3.6(1) eV and is a direct measure of the crystal field splitting.  $\text{NaOsO}_3$  and  $\text{Cd}_2\text{Os}_2\text{O}_7$  have a similar local  $\text{OsO}_6$  octahedral environment, however the  $t_{2g}-e_g$  splitting is 0.9 eV lower in  $\text{NaOsO}_3$  [16]. This indicates that considerations beyond the local  $5d$  octahedral environment are crucial, which is in line with expectations of the importance of the spatially extended  $5d$  orbitals.

The magnetic order and consequently the magnetic exchange interactions are central to the creation of the MIT in  $\text{NaOsO}_3$ . Therefore measuring and modeling the dominant exchange pathways is required to yield a complete picture of the MIT. The crystal size of  $\text{NaOsO}_3$  is currently beyond the limits of inelastic neutron scattering, however RIXS offers a route to quantitatively probe the collective magnetic excitations in  $5d$  systems [17]. The low energy scattering for  $\text{NaOsO}_3$  using high resolution Os RIXS is shown in Fig. 2. Measurements along high symmetry directions shows a single resolution limited inelastic excitation ( $E_A$ ). The excitation, along with the elastic line, were fit with a Gaussian peak shape to follow the dispersion. Fig. 3(a) reveals  $E_A$  is strongly dispersive indicative of a spin-wave excitation. The bandwidth is  $\sim 80$  meV with maxima at the zone boundary along the Z and X direction and a reduced energy at Y. A large spin gap of 58 meV is observed at zone center ( $\Gamma$ ) that signifies the presence of strong anisotropy in  $\text{NaOsO}_3$ .

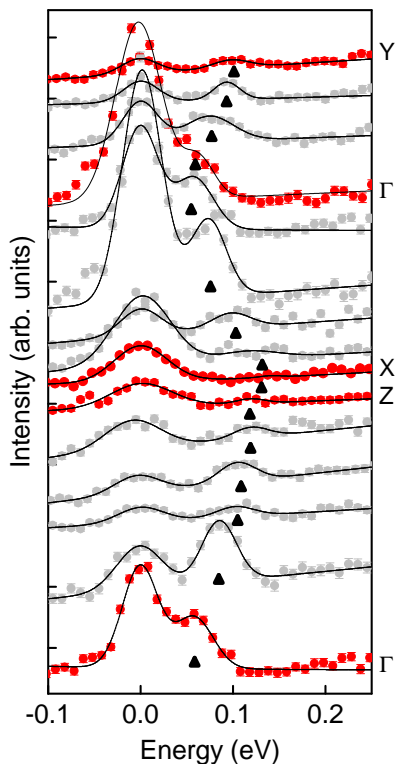


FIG. 2. RIXS measurements of NaOsO<sub>3</sub> at 300 K along high symmetry directions in the Brillouin zone. The line shows the fit to the elastic and inelastic scattering at E<sub>A</sub>, with the position of E<sub>A</sub> indicated by the triangles. The data have been offset to aid comparison.

To provide a quantitative description of the magnetic excitations we invoke a minimal model Hamiltonian with nearest neighbor (nn) and next nearest neighbor (nnn) exchange interactions:

$$\mathcal{H} = J_1 \sum_{nn} \mathbf{S}_i \cdot \mathbf{S}_j + J_2 \sum_{nnn} \mathbf{S}_i \cdot \mathbf{S}_j + \Delta \quad (1)$$

A SOC induced anisotropic term is included to account for the gap. For the case of symmetric exchange anisotropy  $\Delta = \Gamma \sum_{nn, nnn} S_i^z S_j^z$  and for single-ion anisotropy  $\Delta = D \sum (S_z^2)_i$

The RIXS data for NaOsO<sub>3</sub> was modeled within a linear spin wave (LSW) approximation [19] and the results checked against numerical calculations using SpinW [20]. The nominal spin-only value of S=3/2 was used throughout. Fitting the experimental dispersion to equation (1) produces close agreement to both the dispersion and corresponding intensity, Fig. 3, indicating the minimal model Hamiltonian captures the essential features and consequently provides an experimental assignment of the dominant magnetic exchange interactions and their energy. The fitting yields  $J_1=J_2=13.9(5)$  meV and  $\Gamma=1.4(1)$  meV. Allowing  $J_1$  and  $J_2$  to vary independently did not improve the fit, reflecting the pseudo-cubic

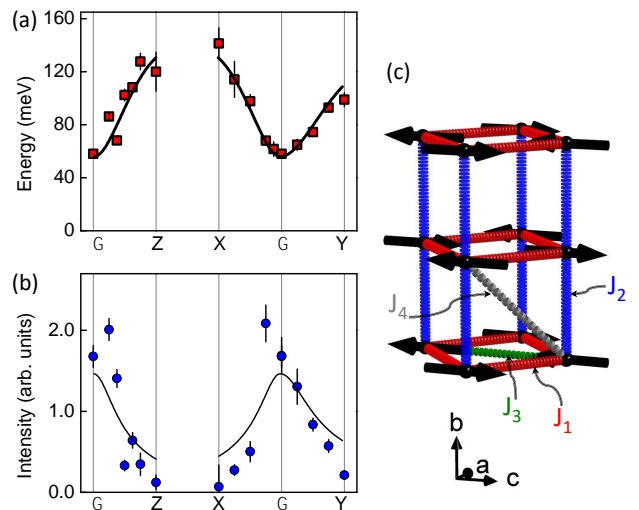


FIG. 3. (a) Measured (squares) and calculated (line) dispersion of E<sub>A</sub> along high symmetry directions. (b) Measured (circles) and calculated (line) intensity of E<sub>A</sub>. (c) The calculations were performed using equation (1), a minimal model Hamiltonian with the exchange interactions  $J_1$  and  $J_2$ .

nature of the structure. Adding a third-nearest neighbor term  $J_3$ , or  $J_3=J_4$  to recover the cubic limit, alters the energy at Z with respect to X, however within resolution the measured energy at X=Z. Therefore we conclude that exchange interactions  $J_3$  and above have a magnitude appreciably less than  $J_1$  or  $J_2$  and limit the Hamiltonian to equation (1). Consequently NaOsO<sub>3</sub> is well described by dominant nearest neighbor magnetic interactions in three dimensions forming a robust G-type antiferromagnetic order in this perovskite. Replacing exchange anisotropy with a single-ion anisotropy ( $D \sum (S_z^2)_i$ ) term yields the same  $J_1$  and  $J_2$  values and  $D=4$  meV.

The mechanism for the spin-gap is effectively disconnected from the magnetic exchange interactions in equation (1). However, the presence of such a large spin-gap is significant in terms of the underlying physics in NaOsO<sub>3</sub>. In particular, all possible mechanisms to open a spin-gap, SIA, the Dzyaloshinskii-Moriya (DM) interaction and exchange anisotropy, require SOC. We briefly consider how the anisotropies influence NaOsO<sub>3</sub>. SIA arises due to a non-cubic environment and in NaOsO<sub>3</sub> the OsO<sub>6</sub> octahedra are weakly trigonally and tetragonally compressed. However, such a large gap due to SIA does not appear consistent with the reduced spin-gaps of 15-20 meV observed in other  $5d^3$  osmates with similar distortions [15]. In NaOsO<sub>3</sub> a non-zero local DM vector exists since the oxygen mediating the superexchange interaction between the two Os sites does not sit at an inversion center. Experimentally there is evidence of weak ferromagnetism [21], however the spin-canting producing this was undetectable with neutron diffraction [7]. This would suggest that the DM interaction, while present, is weak to first or-

der. Exchange anisotropy, a pseudodipolar effect, results as a consequence of second-order SOC effects between neighboring Os ions, and hence is generally weaker than the DM interaction and SIA. However, in  $5d$  systems the extended orbitals result in enhanced collective behavior within the lattice compared to, for example, that which occurs in  $3d$  transition metal oxides. Indeed this was shown in  $\text{NaOsO}_3$  with the observation of an enhanced spin-phonon shift at the MIT due to the extended Os orbitals [13].

The measurement of a large-spin gap indicates that SOC is required in a complete description of  $\text{NaOsO}_3$ . The magnitude of SOC scales with the atomic number, therefore in  $5d^3$  osmates it is comparable to  $5d^5$  iridates. However, when describing the properties of  $\text{NaOsO}_3$  the role of SOC has only been required to be included as a perturbation [6, 7, 9–13]. Conversely for  $5d^5$  iridates SOC is necessary to describe both magnetism and the insulating state. This has created an apparent dichotomy between the effect of SOC, particularly when considering the divergent electronic ground states indicated from the RIXS spectra between  $5d^3$  and  $5d^5$ . A first approximation is that the altered electronic occupancy causes an increased Hund's coupling in  $5d^3$  systems favoring a quenching of orbital momentum. However, the broad scattering observed for  $E_B$  in Fig. 1 indicates underlying splitting of the  $t_{2g}$  orbitals, either through structural distortions or SOC or a combination of both. One consequence of an increased role of SOC in  $\text{NaOsO}_3$  was considered theoretically to reduce the effective  $U$  and place the system closer to the itinerant limit description of magnetism [22]. However, the agreement of the minimal-model Hamiltonian, based on localized spins, to the RIXS spectra would suggest that the behavior of  $\text{NaOsO}_3$  appreciably departs from being fully itinerant. Indeed this would be expected even within the mean-field Hartree-Fock description used by Slater to describe a magnetic MIT since at the transition local moments are necessarily formed [23]. While in a pure Slater description this would be treated by self-consistent single electron theory, at least to a good approximation the behavior can be described by a Heisenberg model and places  $\text{NaOsO}_3$  on the boundary between local-moment and itinerant magnetism.

The  $5d$  orbital and collective magnetic excitations in  $\text{NaOsO}_3$  have been probed with RIXS. Well-defined spin waves were observed and described within linear spin wave theory using a minimal model Hamiltonian that captured the essential features. Nearest and next nearest Heisenberg exchange interactions of  $J_1=J_2=13.9$  meV were found to describe the dispersion, indicating strong three-dimensional magnetic interactions. The presence of significant anisotropy in the system was observed with the measurement of a large spin gap of 58 meV. This is a direct consequence of intrinsically strong SOC in this  $5d$  compound, however the role of SOC on the ground

state departs from  $5d^5$  iridates. In terms of the mechanism of the MIT the results support a three-dimensional magnetically driven route, consistent with the general scenario proposed by Slater. The Hamiltonian presented here provides the magnetic interaction energy scales and their pathways required to describe the MIT. Moreover, the presence of SOC and the influence this has within a system with extended orbitals and strong hybridization has to be considered as playing an important role when considering the collective interactions and the MIT.

A. D. C. thanks A. Taylor for useful discussions. We thank C. Henriquet and R. Verbeni at the ESRF for design and manufacture of the high-temperature stage. Preliminary measurements were performed at 9-ID-B and 30-ID (MERIX), APS, which is a U.S. Department of Energy (DOE) Office of Science User Facility operated for the DOE Office of Science by Argonne National Laboratory under Contract No. DE-AC02-06CH11357. The research at ORNL was sponsored by the Scientific User Facilities Division, Office of Basic Energy Sciences, U.S. Department of Energy. Work in London was supported by EPSRC. J. G. V. would like to thank UCL and EPFL for financial support via a UCL Impact Studentship. X. L. acknowledges financial support from MOST (No. 2015CB921302) and CAS (No: XDB07020200) of China.

---

\* caldersa@ornl.gov

† j.vale@ucl.ac.uk

- [1] M. Imada, A. Fujimori, and Y. Tokura, *Rev. Mod. Phys.* **70**, 1039 (1998).
- [2] W. Witczak-Krempa, G. Chen, Y. B. Kim, and L. Balents, *Annual Review of Condensed Matter Physics* **5**, 57 (2014).
- [3] B. J. Kim, H. Ohsumi, T. Komesu, S. Sakai, T. Morita, H. Takagi, and T. Arima, *Science* **323**, 1329 (2009).
- [4] D. Mandrus, J. R. Thompson, R. Gaal, L. Forro, J. C. Bryan, B. C. Chakoumakos, L. M. Woods, B. C. Sales, R. S. Fishman, and V. Keppens, *Phys. Rev. B* **63**, 195104 (2001).
- [5] J. Yamaura, K. Ohgushi, H. Ohsumi, T. Hasegawa, I. Yamauchi, K. Sugimoto, S. Takeshita, A. Tokuda, M. Takata, M. Udagawa, M. Takigawa, H. Harima, T. Arima, and Z. Hiroi, *Phys. Rev. Lett.* **108**, 247205 (2012).
- [6] Y. G. Shi, Y. F. Guo, S. Yu, M. Arai, A. A. Belik, A. Sato, K. Yamaura, E. Takayama-Muromachi, H. F. Tian, H. X. Yang, J. Q. Li, T. Varga, J. F. Mitchell, and S. Okamoto, *Phys. Rev. B* **80**, 161104 (2009).
- [7] S. Calder, V. O. Garlea, D. F. McMorrow, M. D. Lumsden, M. B. Stone, J. C. Lang, J.-W. Kim, J. A. Schlueter, Y. G. Shi, K. Yamaura, Y. S. Sun, Y. Tsujimoto, and A. D. Christianson, *Phys. Rev. Lett.* **108**, 257209 (2012).
- [8] J. C. Slater, *Phys. Rev.* **82**, 538 (1951).
- [9] Y. Du, X. Wan, L. Sheng, J. Dong, and S. Y. Savrasov, *Phys. Rev. B* **85**, 174424 (2012).
- [10] M.-C. Jung, Y.-J. Song, K.-W. Lee, and W. E. Pickett,

- Phys. Rev. B **87**, 115119 (2013).
- [11] I. L. Vecchio, A. Perucchi, P. Di Pietro, O. Limaj, U. Schade, Y. Sun, M. Arai, K. Yamaura, and S. Lupi, Scientific Reports **3**, 2990 (2013).
- [12] S. Middey, S. Debnath, P. Mahadevan, and D. D. Sarma, Phys. Rev. B **89**, 134416 (2014).
- [13] S. Calder, J. H. Lee, M. B. Stone, M. D. Lumsden, J. C. Lang, M. Feyngenson, Z. Zhao, J.-Q. Yan, Y. G. Shi, Y. S. Sun, Y. Tsujimoto, K. Yamaura, and A. D. Christianson, Nature Communications **6**, 8916 (2015).
- [14] E. Kermarrec, C. A. Marjerrison, C. M. Thompson, D. D. Maharaj, K. Levin, S. Kroecker, G. E. Granroth, R. Flacau, Z. Yamani, J. E. Greedan, and B. D. Gaulin, Phys. Rev. B **91**, 075133 (2015).
- [15] A. E. Taylor, R. Morrow, R. S. Fishman, S. Calder, A. I. Kolesnikov, M. D. Lumsden, P. M. Woodward, and A. D. Christianson, Phys. Rev. B **93**, R220408 (2016).
- [16] S. Calder, J. G. Vale, N. A. Bogdanov, X. Liu, C. Donnerer, M. H. Upton, D. Casa, A. H. Said, M. D. Lumsden, Z. Zhao, J. Q. Yan, D. Mandrus, S. Nishimoto, J. van den Brink, J. P. Hill, D. F. McMorrow, and A. D. Christianson, Nature Communications **7**, 11651 (2016).
- [17] J. Kim, D. Casa, M. H. Upton, T. Gog, Y.-J. Kim, J. F. Mitchell, M. van Veenendaal, M. Daghofer, J. van den Brink, G. Khaliullin, and B. J. Kim, Phys. Rev. Lett. **108**, 177003 (2012).
- [18] M. Moretti Sala, S. Boseggia, D. F. McMorrow, and G. Monaco, Phys. Rev. Lett. **112**, 026403 (2014).
- [19] Diagonalizing the Hamiltonian in equation (1) within a LSW approximation gives the spin wave energy  $\omega$ :  $\omega = S\sqrt{D - X - Y}$ , where  $D = 36\Delta^2 + 48\Delta J_1 + 24\Delta J_2 + 12J_1^2 + 2J_2^2 + 16J_1J_2$ ,  $X = 4J_1^2 \cos 2\pi h + 2J_2^2 \cos 2\pi h + 4J_1^2 \cos 2\pi l$ ,  $Y = 2J_1^2 \cos [2\pi(h-l)] + 2J_1^2 \cos [2\pi(h+l)] + 16J_1J_2 \cos \pi h \cos \pi k \cos \pi l$ . In a similar fashion the intensity can be expressed by:  $S(q, \omega) = S \left[ \frac{D - (X - Y)}{D - (X + Y)} \right] \delta(\omega, \omega_q)$ .
- [20] S. Toth and B. Lake, Journal of Physics: Condensed Matter **27**, 166002 (2015).
- [21] Y. G. Shi, Y. F. Guo, S. Yu, M. Arai, A. A. Belik, A. Sato, K. Yamaura, E. Takayama-Muromachi, H. F. Tian, H. X. Yang, J. Q. Li, T. Varga, J. F. Mitchell, and S. Okamoto, Phys. Rev. B **80**, 161104 (2009).
- [22] B. Kim, P. Liu, Z. Ergonenc, A. Toschi, S. Khmelevskiy, and C. Franchini, arXiv:1601.03310 (2016).
- [23] F. Gebhard, *The Mott Metal-Insulator Transition* (Springer, Berlin, 1997).